122

SATELLITE & MESOMETEOROLOGY RESEARCH PROJECT

Department of the Geophysical Sciences
The University of Chicago

ANALYSIS OF ANVIL GROWTH FROM ATS PICTURES

by

Yun-Mei Chang

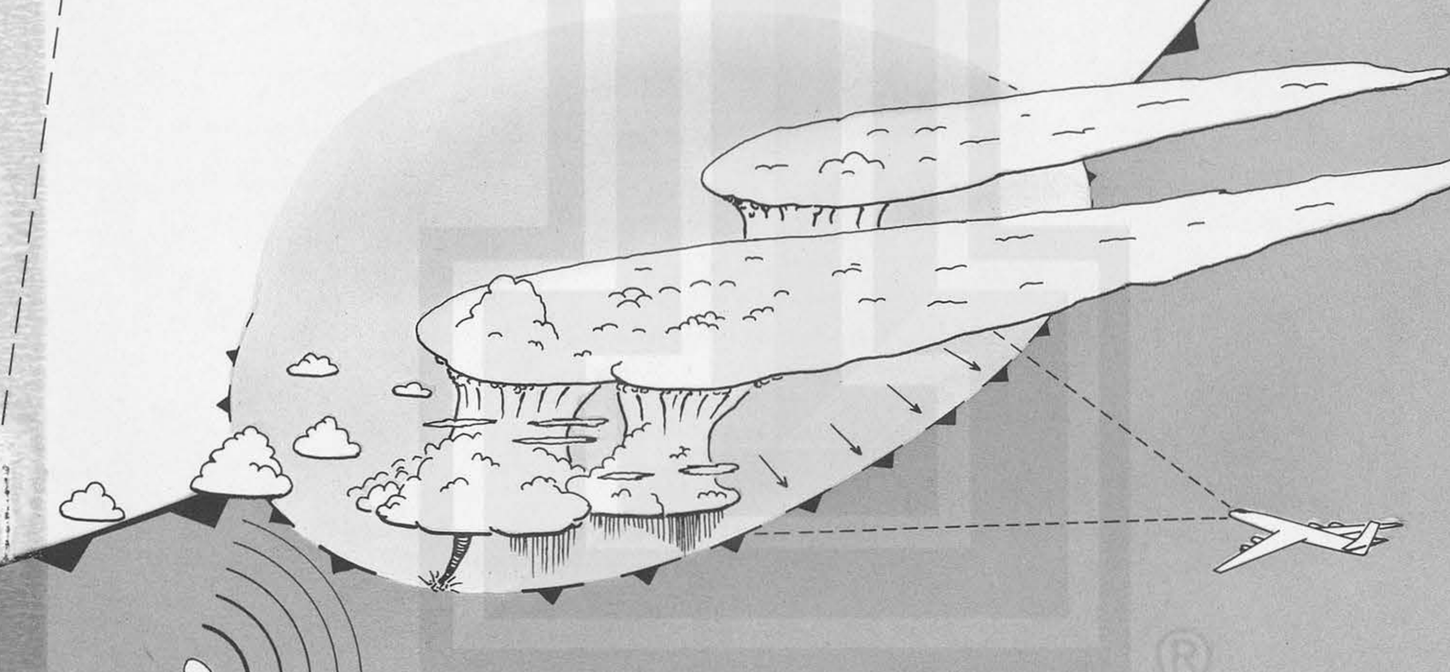

SMRP Research Paper

Number 122
July 1974

MESOMETEOROLOGY PROJECT --- RESEARCH PAPERS

1.* Report on the Chicago Tornado of March 4, 1961 - Rodger A. Brown and Tetsuya Fujita

2.* Index to the NSSP Surface Network - Tetsuya Fujita

3.* Outline of a Technique for Precise Rectification of Satellite Cloud Photographs - Tetsuya Fujita

4.* Horizontal Structure of Mountain Winds - Henry A. Brown

5.* An Investigation of Developmental Processes of the Wake Depression Through Excess Pressure Analysis of Nocturnal Showers - Joseph L. Goldman

6.* Precipitation in the 1960 Flagstaff Mesometeorological Network - Kenneth A. Styber

7.** On a Method of Single- and Dual-Image Photogrammetry of Panoramic Aerial Photographs - Tetsuya Fujita

8. A Review of Researches on Analytical Mesometeorology - Tetsuya Fujita

9.* Meteorological Interpretations of Convective Nephsystems Appearing in TIROS Cloud Photographs - Tetsuya Fujita, Toshimitsu Ushijima, William A. Hass, and George T. Dellert, Jr.

10.* Study of the Development of Prefrontal Squall-Systems Using NSSP Network Data - Joseph L. Goldman

11. Analysis of Selected Aircraft Data from NSSP Operation, 1962 - Tetsuya Fujita

12. Study of a Long Condensation Trail Photographed by TIROS I - Toshimitsu Ushijima

13. A Technique for Precise Analysis of Satellite Data; Volume I - Photogrammetry (Published as MSL Report No. 14) - Tetsuya Fujita

14. Investigation of a Summer Jet Stream Using TIROS and Aerological Data - Kozo Ninomiya

15. Outline of a Theory and Examples for Precise Analysis of Satellite Radiation Data - Tetsuya Fujita

16. Preliminary Result of Analysis of the Cumulonimbus Cloud of April 21, 1961 - Tetsuya Fujita and James Arnold

17. A Technique for Precise Analysis of Satellite Photographs - Tetsuya Fujita

18.* Evaluation of Limb Darkening from TIROS III Radiation Data - S.H.H. Larsen, Tetsuya Fujita, and W.L. Fletcher

19. Synoptic Interpretation of TIROS III Measurements of Infrared Radiation - Finn Pedersen and Tetsuya Fujita

20.* TIROS III Measurements of Terrestrial Radiation and Reflected and Scattered Solar Radiation - S.H.H. Larsen, Tetsuya Fujita, and W.L. Fletcher

21. On the Low-level Structure of a Squall Line - Henry A. Brown

22.* Thunderstorms and the Low-level Jet - William D. Bonner

23.* The Mesoanalysis of an Organized Convective System - Henry A. Brown

24. Preliminary Radar and Photogrammetric Study of the Illinois Tornadoes of April 17 and 22, 1963 - Joseph L. Goldman and Tetsuya Fujita

25. Use of TIROS Pictures for Studies of the Internal Structure of Tropical Storms - Tetsuya Fujita with Rectified Pictures from TIROS I Orbit 125, R/O 128 - Toshimitsu Ushijima

26. An Experiment in the Determination of Geostrophic and Isallobaric Winds from NSSP Pressure Data - William Bonner

27. Proposed Mechanism of Hook Echo Formation - Tetsuya Fujita with a Preliminary Mesosynoptic Analysis of Tornado Cyclone Case of May 26, 1963 - Tetsuya Fujita and Robbi Stuhmer

28. The Decaying Stage of Hurricane Anna of July 1961 as Portrayed by TIROS Cloud Photographs and Infrared Radiation from the Top of the Storm - Tetsuya Fujita and James Arnold

29. A Technique for Precise Analysis of Satellite Data, Volume II - Radiation Analysis, Section 6. Fixed-Position Scanning - Tetsuya Fujita

30. Evaluation of Errors in the Graphical Rectification of Satellite Photographs - Tetsuya Fujita

31. Tables of Scan Nadir and Horizontal Angles - William D. Bonner

32. A Simplified Grid Technique for Determining Scan Lines Generated by the TIROS Scanning Radiometer - James E. Arnold

33. A Study of Cumulus Clouds over the Flagstaff Research Network with the Use of U-2 Photographs - Dorothy L. Bradbury and Tetsuya Fujita

34. The Scanning Printer and Its Application to Detailed Analysis of Satellite Radiation Data - Tetsuya Fujita

35. Synoptic Study of Cold Air Outbreak over the Mediterranean using Satellite Photographs and Radiation Data - Aasmund Rabbe and Tetsuya Fujita

36. Accurate Calibration of Doppler Winds for their use in the Computation of Mesoscale Wind Fields - Tetsuya Fujita

37. Proposed Operation of Intrumented Aircraft for Research on Moisture Fronts and Wake Depressions - Tetsuya Fujita and Dorothy L. Bradbury

38. Statistical and Kinematical Properties of the Low-level Jet Stream - William D. Bonner

39. The Illinois Tornadoes of 17 and 22 April 1963 - Joseph L. Goldman

40. Resolution of the Nimbus High Resolution Infrared Radiometer - Tetsuya Fujita and William R. Bandeen

41. On the Determination of the Exchange Coefficients in Convective Clouds - Rodger A. Brown

* Out of Print
** To be published

(Continued on back cover)

ANALYSIS OF ANVIL GROWTH FROM ATS PICTURES

by

Yun-Mei Chang
Department of the Geophysical Sciences
The University of Chicago

SMRP Research Paper Number 122
July 1974

Research supported by the Atmospheric Sciences Section, National Science Foundation, Grant GA-41845, and by the National Oceanic and Atmospheric Administration, Grant No. 04-4-158-1.

ANALYSIS OF ANVIL GROWTH FROM ATS PICTURES

Yun-Mei Chang
Department of the Geophysical Sciences
The University of Chicago

ABSTRACT

The growth of two fast-spreading anvil clouds is studied from a sequence of ATS-III pictures on July 26, 1969. The anvil boundaries and cloud elements on the anvil edges are traced. Anvil boundaries are drawn at one-hour intervals and the cloud motion fields are thus calculated. The results are related to a moving tropical depression with a warm core anticyclone aloft. It is suggested that the tracking of anvil boundaries from satellite pictures is useful in obtaining a reliable and accurate upper-divergence field over disturbances in the tropics, and, thus, makes it possible to obtain a better comprehension of the mechanism in tropical circulations.

1. INTRODUCTION

The existence of an upper divergence field at tropopause level in the tropics has been found by many researchers. This upper divergence is manifested by fast-spreading anvil clouds. Studies of the outflow field associated with these clouds have been used to investigate the characteristics of thunderstorms as well as tornadoes. Among others, the spreading rate of anvil clouds in relation to the severe storms was studied by Fujita and Bradbury (1969). Sikdar et al. (1970) suggested that the cloud divergence at the top of an intense convection zone can be calculated to estimate the probable severity of a particular weather phenomenon for the next few hours. The growth of anvils in the thunderstorm clusters was also measured by Purdom (1971) by using the ATS imagery, and a pause in the anvil growth was found preceding the tornado.

In this report, the emphasis is placed upon the determination of the anvil area by tracking the anvil boundaries from a series of ATS time-lapse pictures which was a concept pioneered by Fujita (1974). The cloud elements of the anvil edge are also tracked and the cloud velocities are thus calculated by the METRACOM System developed at the University of Chicago. In an attempt to learn more about the traits of the spreading anvils, the hourly analysis of the growth of the anvil area, the upper divergence vorticity, outflow and circulation fields are obtained. The main purpose of the study is to examine the relation between the characteristics of the anvil growth and the development and movement of a large-scale weather system.

2. TRACKING OF ANVIL BOUNDARIES

A sequence of nineteen ATS-III pictures for July 26, 1969 is used, which has first frame time of 1233 Z and last frame time of 1903 Z as shown in Fig. 1. To identify the locations of anvil clouds, pictures with clear landmarks are selected. The anvil clouds shown on the pictures are very bright with prominent cirriform clouds around. Strong updrafts under the bright anvil top are not detected from the satellite photographs. Anvil boundaries are traced manually from the ATS pictures which have been projected and enlarged to identical size on a film projector.

Two growing anvils are studied. One is centered initially around 15°N and 59° W (anvil A), while the other (anvil B) is around 11.5° N and 65° W. Anvil A, which is rectangular-shaped at the beginning period, has a dimension about 74 km in length and 46 km in width; by the end period it is almost elliptically-shaped with major and minor axes of 322 km and 276 km, respectively. Anvil B has a rectangular dimension of about 64 km in length and 43 km in width at the beginning and again an elliptical shape, with major and minor axes of 150 km and 111 km, respectively, toward the end period is noted. The time interval between frames for the nineteen pictures averages 13 minutes, with the exception of the two frames before the last frame which have about a two-hour interval. The method employed in tracing the boundaries of anvils A and B is such that a set consisting of every other frame, beginning with the first picture and including the last three frames is traced first. Then the remaining set is traced next on the same sheet.

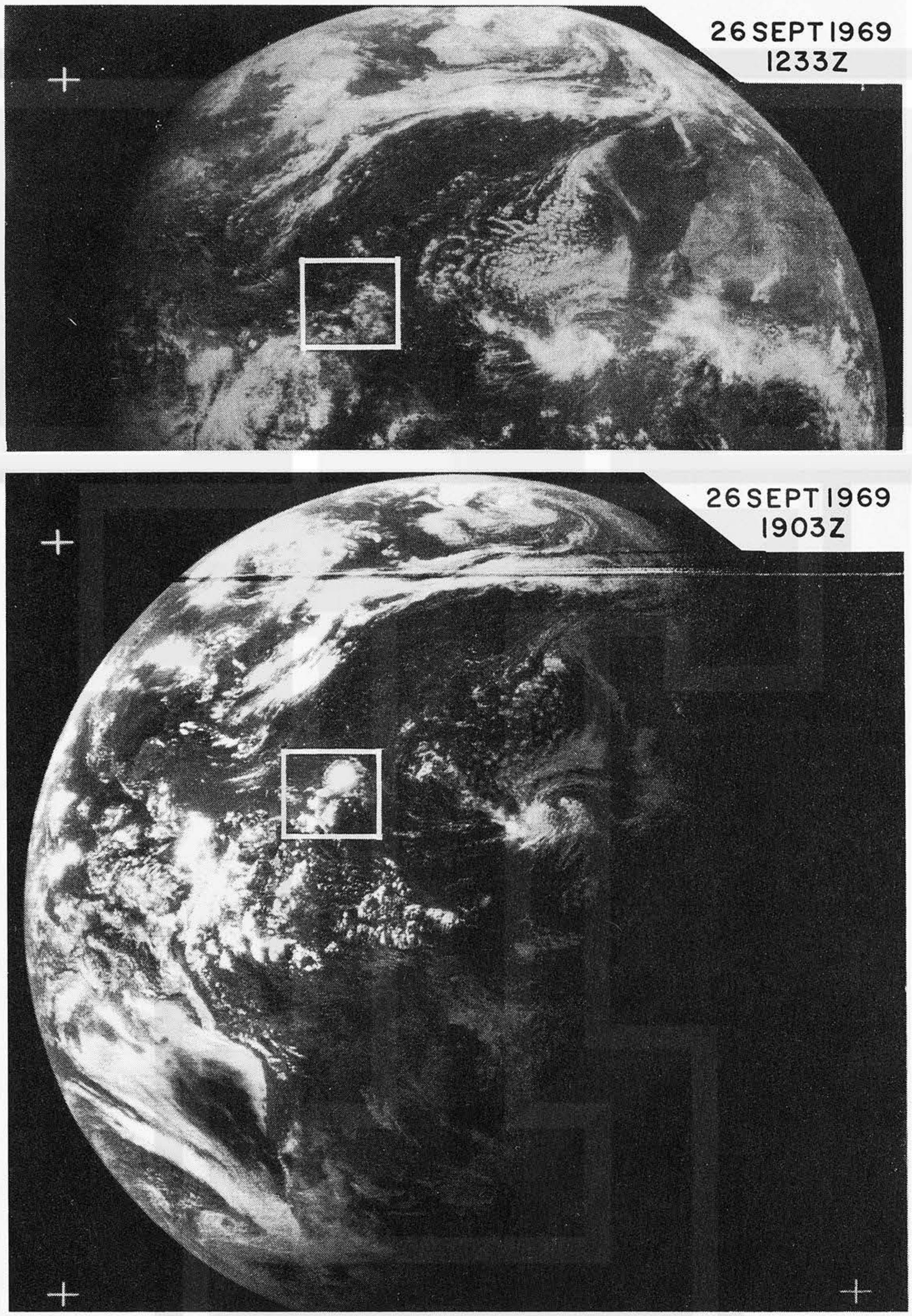

Fig. 1. The first frame, 1233Z (top portion), and last frame, 1903Z (bottom portion), of the satellite picture sequence for July 26, 1969.

While tracking the boundaries, it is noticed that the anvil growth is not symmetric. Anvil A is composed of two groups of cloud clusters. A newly formed cloud cluster grows and forms the right part of anvil A. This right side cloud cluster spreads to the east, since the cloud cluster on the left side of anvil A forms a sort of restraining block as it simultaneously expands westward. The boundaries thus tracked include both the newly-formed and pre-formed cloud clusters. The west edge of anvil A expanded much faster than the east edge. It started growing at 1350 Z and expanded quite rapidly until about 1838 Z; then the expansion rate decreased and the edge became vague and disappeared after 1903 Z.

Anvil B has been in the growth stage since the time of the first frame, expanding and moving at the same time. The edge of anvil B became fuzzy by 1507 Z, then disappeared and new clouds formed to the north afterwards.

Figure 2 shows the location of the expanding anvils A and B on July 26, 1969. The shaded portions are the initial cloud configurations while the closed curves indicate the expanded areas. The observed 200 mb winds at 1200 Z are plotted. The track of a tropical depression for this day, which will be discussed in Section 5, is also shown.

3. EXPANSION OF ANVIL CLOUDS

In addition to the anvil boundaries, the trajectories of the anvil edge are also obtained by tracking the motion of cloud elements from one frame to the next. Anticyclonic curvature of cloud trajectories are found on both anvils A and B. This is expected in the upper divergence level where a storm affects the area at lower level.

Hourly analyses of the anvil boundaries are drawn and the velocities of cloud motions are then calculated by the METRACOM System developed at SMRP, The University of Chicago. This system combines the manual tracking of cloud motions from time-lapse movie loop by trained meteorologist and the computer calculations of the cloud velocities after digital data of cloud positions are digitized from an electronic digitizer. For detailed discussion of METRACOM System, see the report by Chang et al. (1973).

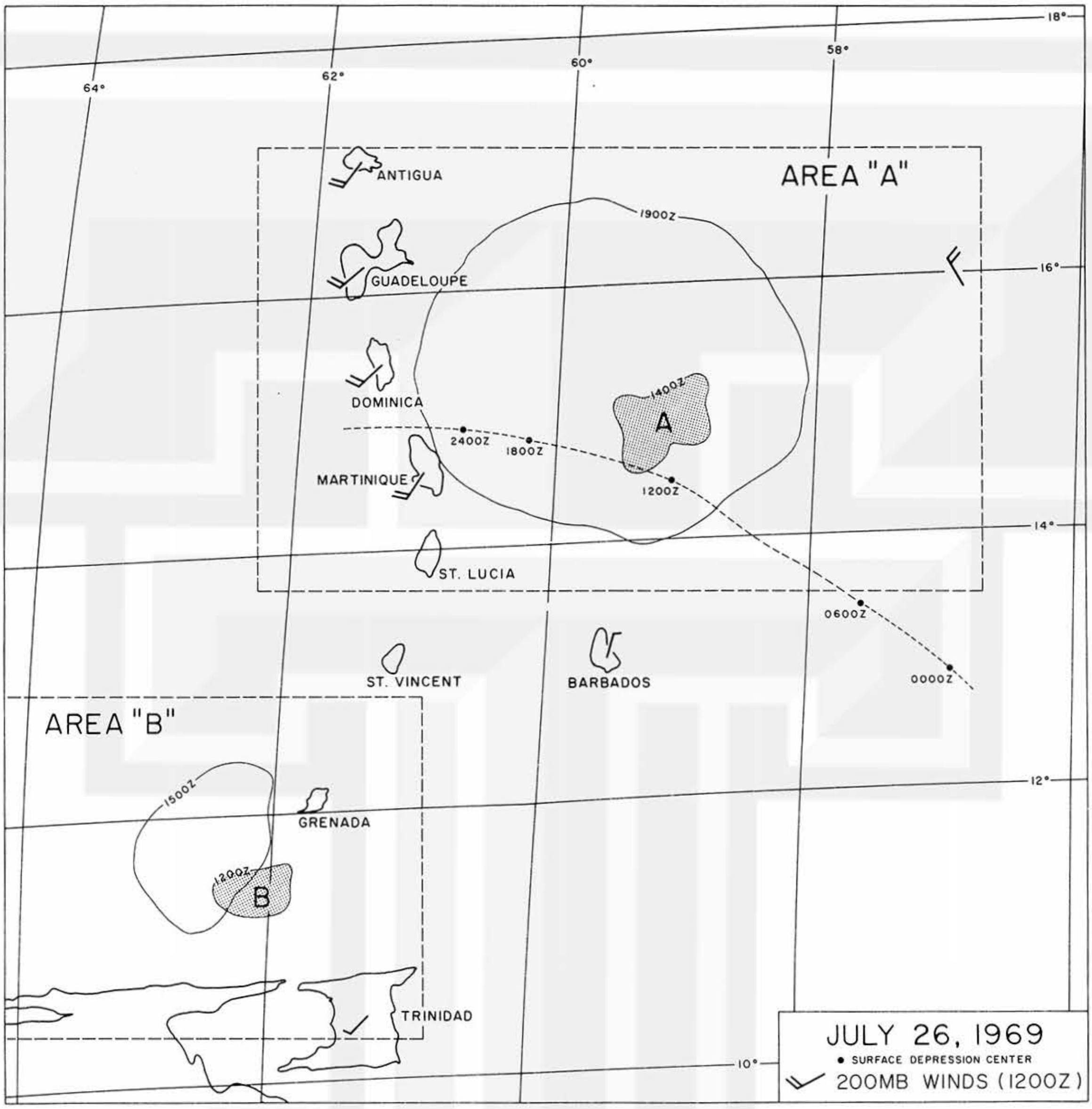

Fig. 2. The boundaries at beginning hour and end hour of expanding anvils A and B together with the 200 mb data at 1200 Z for July 26, 1969. Full circles denote the surface depression center.

The computed cloud velocities together with the hourly boundaries for anvil A are shown in Fig. 3. The cloud velocities reveal a faster expansion over the western and northwestern edge and slower expansion to the eastern and southeastern edge. The right part of the anvil which is a newly-formed cloud cluster, as discussed in Section 2, has an envelope which is shown by a dashed line. The maximum speed of the cloud element in anvil A is 32 kts toward north-northwest between 1600 and 1700 Z,

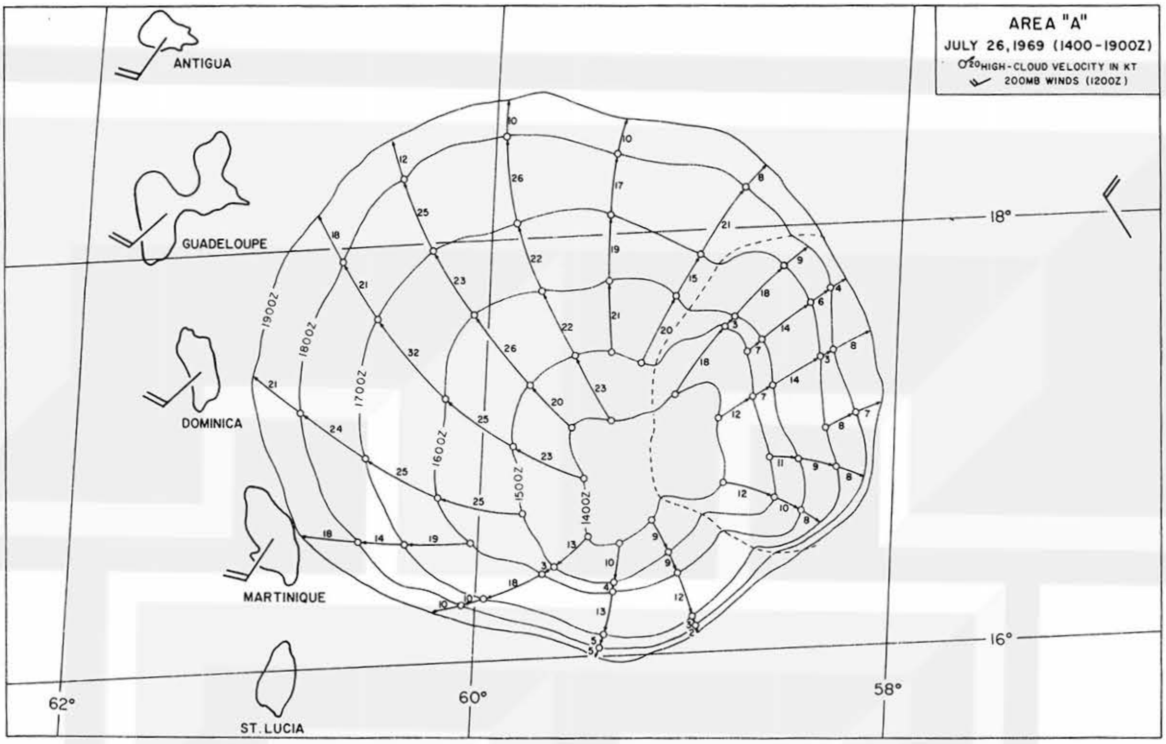

Fig. 3. Hourly analysis of expanding anvil cloud A. Anvil boundaries and cloud velocities at the anvil edge for area "A" in Fig. 2 are shown. Dashed line is the envelope of a newly formed cloud cluster at the right portion of the anvil.

while the minimum speed is 2 kts towards the south-southeast between 1800 and 1900 Z. The whole anvil has a tendency to expand toward the northwest direction and the expansion speed of the anvil edge increased continuously from 1400 Z until 1800 Z, and thereafter decreased. This corresponds to what has been observed when tracking the anvil boundaries and is discussed in Section 2.

Figure 4 is the hourly analysis of the boundary and computed cloud velocities for anvil B. Cloud computations in anvil B show a maximum speed of 27 kts towards the north-northwest direction on its northwest edge between 1300 and 1400 Z, and a minimum speed of 2 kts toward the northwest direction on its eastern edge between 1200 and 1300 Z. The anvil edge increased its speed from 1200 Z, reached its maximum speed some time between 1300 and 1400 Z, then decreased its speed afterwards. This also corresponds to that observed when tracking the boundaries. The motion of

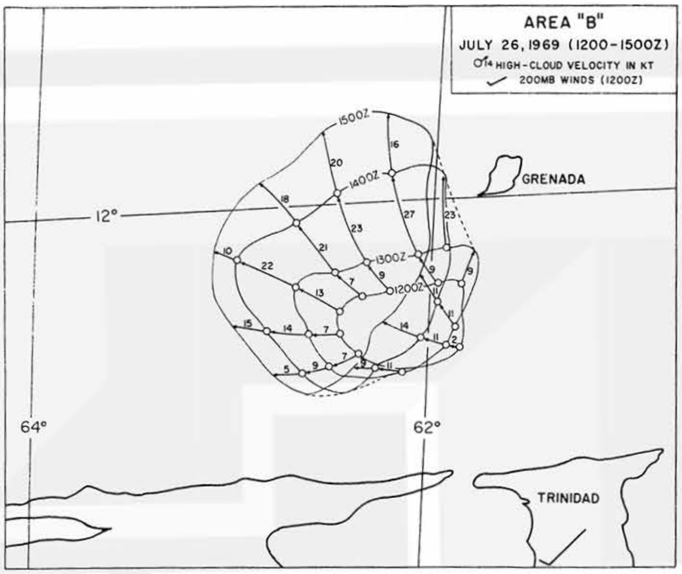

Fig. 4. Hourly analysis of expanding anvil cloud B. Anvil boundaries and cloud velocities at the anvil edge for area "B" in Fig. 2 are shown. Dashed lines denote the envelope of the anvil.

anvil B, different from that of anvil A, included a movement toward the northwest besides expansion in the same direction as discussed in Section 2. The dashed line is its envelope. This may be due to the large scale flow at that level. A contour analysis for 1350 Z to 1454 Z at 200 mb, taken from Chang and Tecson (1974) is shown in Fig. 5. The large scale pattern reveals a southeasterly flow over the anvil areas.

4. KINEMATIC ANALYSES OF ANVIL GROWTH

Figure 6 is the hourly change of anvil A and anvil B areas from 1200 Z to 1900 Z. The areas were measured by a planimeter. The fast spreading of the anvils can be seen from their area growth. For anvil A, however, there is a noticeable decrease of the area growth rate in the last hour. This indicates that anvil A is dying out at that time.

The hourly area mean divergence and mean vorticity are obtained by using the computed cloud velocities. They are calculated by the two-dimensional Gauss theorem and Stokes theorem, namely, by the following formulas

$$\text{mean divergence} = \overline{\nabla\cdot V} = \frac{1}{A}\oint V_n \times d\vec{s}$$

$$\text{mean vorticity} = \overline{\nabla\times V} = \frac{1}{A}\oint V_t \cdot d\vec{s}$$

where "—" represents the area mean, A is the anvil area, V_n and V_t denote the normal and tangential components of cloud velocity along the anvil boundary, respectively, and $d\vec{s}$ is a small element along the anvil boundary. The mean divergence and mean vorticity for every hour are shown in Fig. 7 and Fig. 8, respectively. The anticyclonic vorticity for both anvil A and anvil B have a much smaller order of magnitude, about 1 hr^{-1} . This indicates that the anvils have much more expansion motion than rotation. Except for the 1st hour for anvil B, both mean divergence field and mean vorticity field for both anvils have a tendency of decreasing with time.

The outflow and circulation along the hourly boundaries are also calculated by using the cloud velocities for each hour and are shown in Fig. 9 and Fig. 10, respectively. Both figures exhibit intensification during the beginning hours and then weakening later, since the anvils are dying out eventually. Again, the circulation field is comparably smaller than the outflow field by about one order of magnitude.

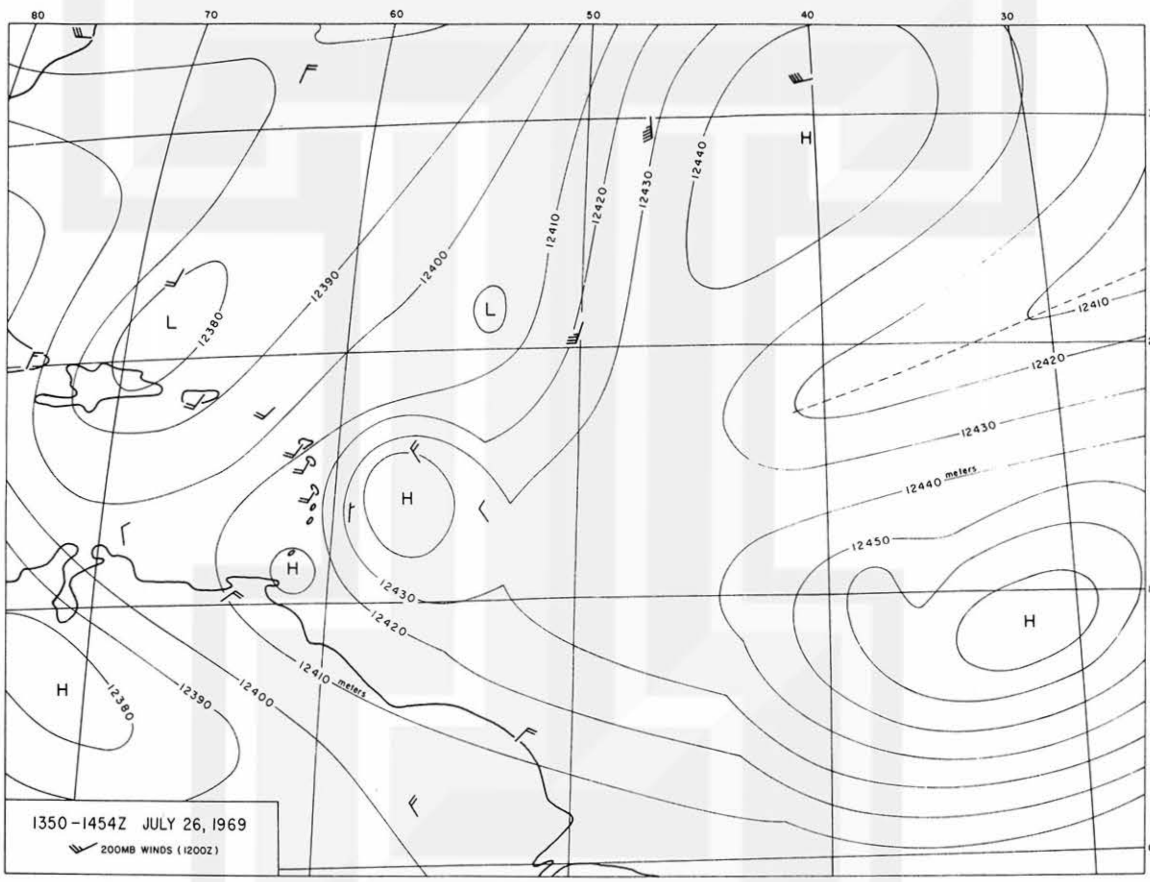

Fig. 5. 200 mb contour analysis for July 26, 1969 (1350-1454 Z) from the calculated high-cloud velocity field and the observed wind data at 1200 Z for the area covered by both anvils A and B.
(From Chang and Tecson, 1974)

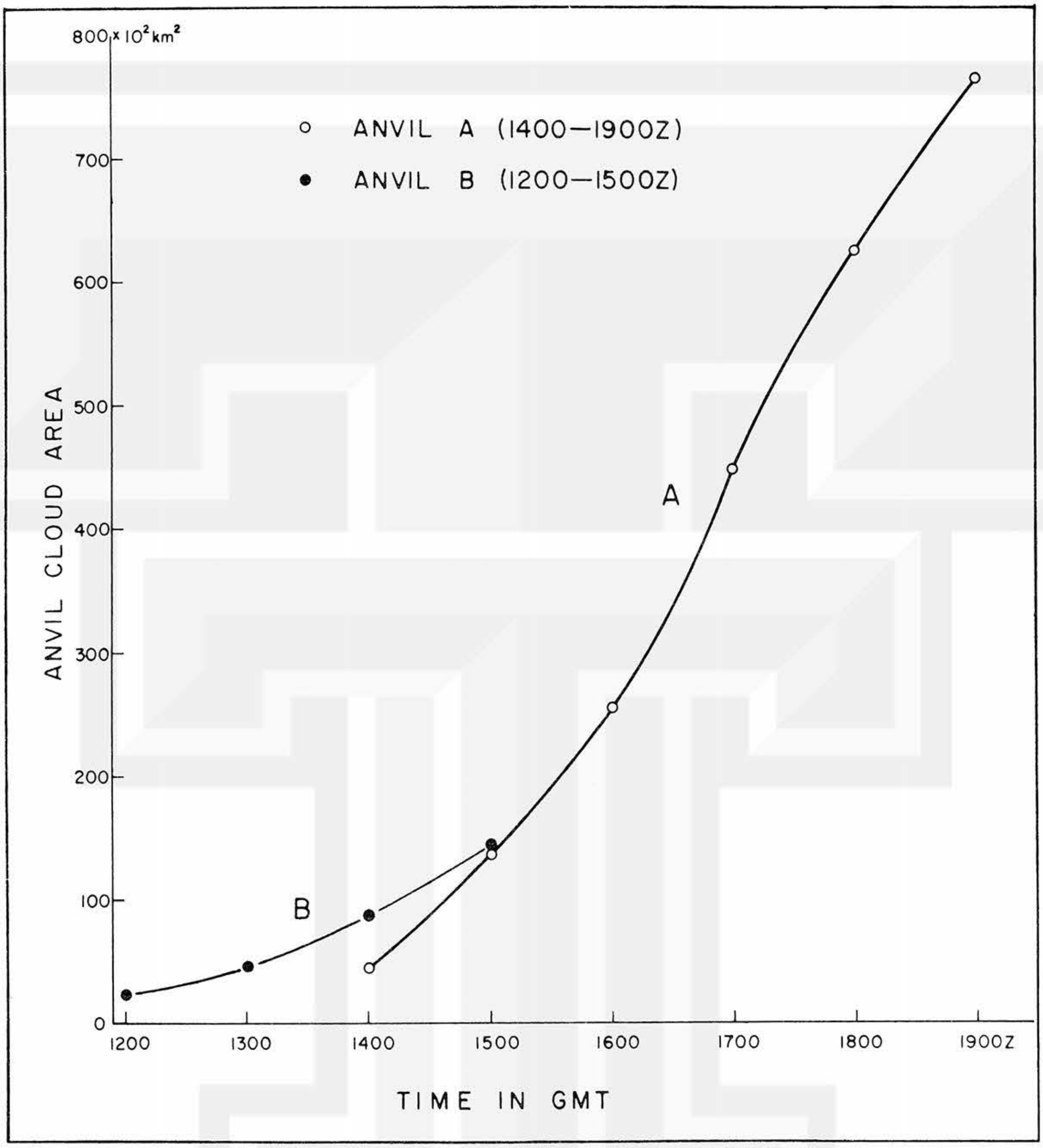

Fig. 6. Areas covered by expanding anvil clouds A and B for July 26, 1969.

5. ANVIL GROWTH IN RELATION TO THE CHARACTERISTICS OF LARGE-SCALE WEATHER SYSTEM

From the aircraft and ship reports, a tropical depression was located near the vicinity east of Martinique and north of Barbados on July 26, 1969. A weak anti-cyclone was superimposed over the depression at upper level. This very well-defined circulation was a warm core system which extended throughout the lower and middle

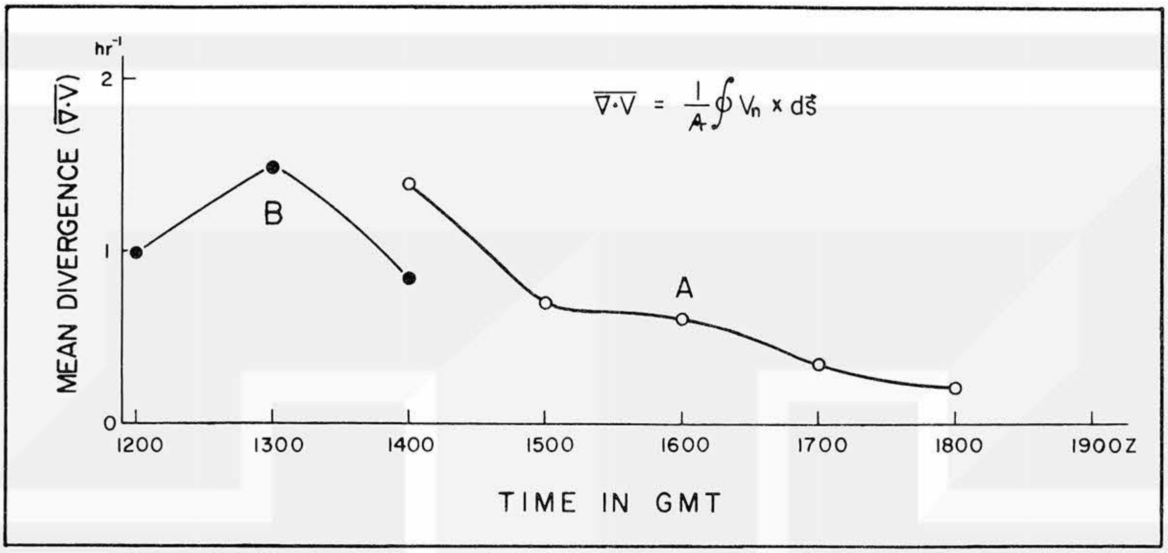

Fig. 7. The area mean divergence of anvils A and B for July 26, 1969.

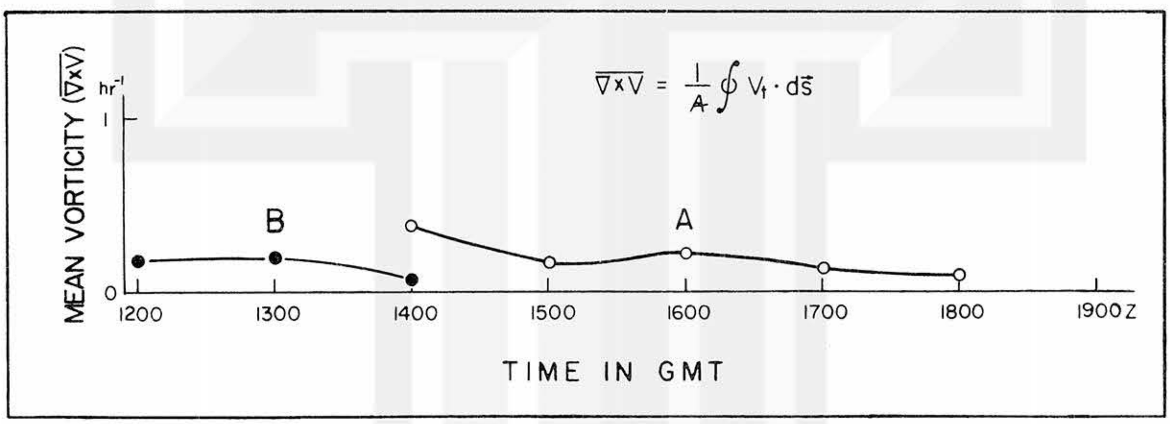

Fig. 8. The area mean vorticity of anvils A and B for July 26, 1969.

troposphere. The convection was very organized in this system. A preliminary analysis was reported by Fernandez-Partagas and Estoque (1970).

The vertical time cross section of wind at Barbados for 1200 Z, 1500 Z, 1800 Z, 2100 Z and 2400 Z, July 26, 1969 are shown in Fig. 11. During the period, the wind at lower troposphere over Barbados showed a marked wind shift from the southwest to the southeast direction with maximum surface wind speed sometime after 1500Z but closer to 1800 Z. This can be closely associated with the cyclonic circulation moving from northeast of Barbados, passing through the north around 1400 Z as it moved to the northwest of Barbados. The cirrus bands observed over Barbados at 1200 Z are associated with the cyclonic system located to the northeast. The sounding at Barbados at 1200 Z, July 26, 1969 is shown in Fig. 12. The southeast winds at 10.5 km are due to the anticyclone superimposed over the depression.

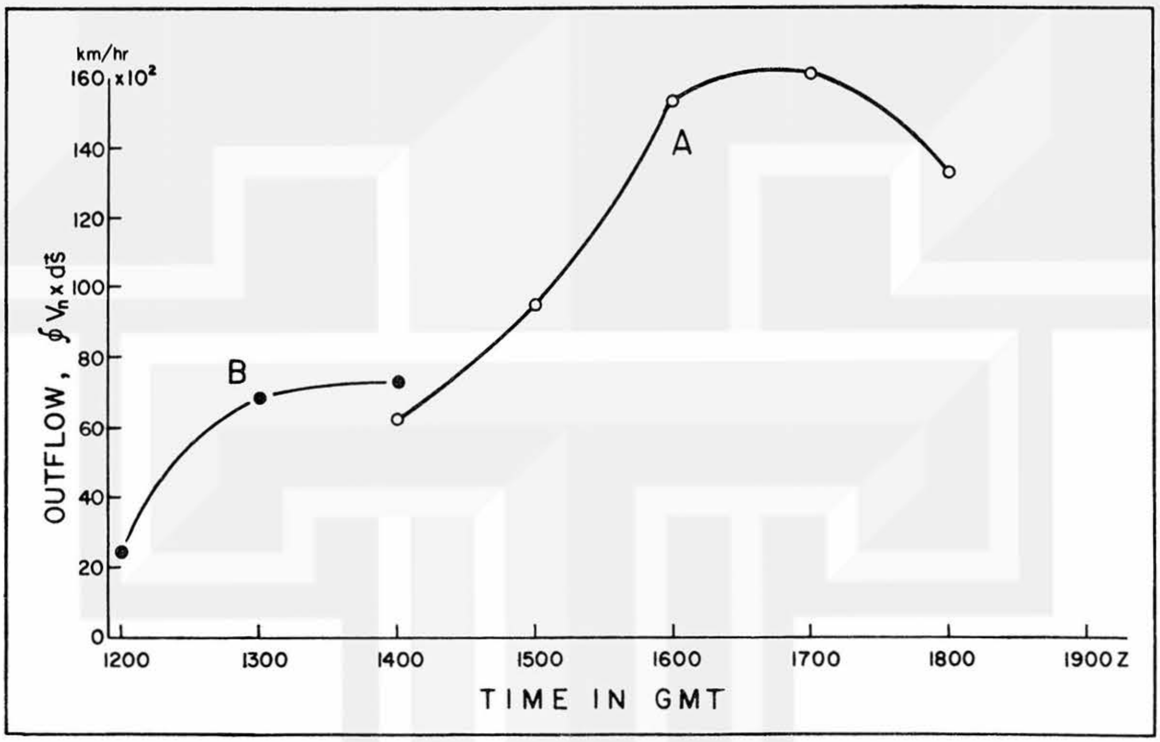

Fig. 9. The outflow from the boundaries of anvils A and B for July 26, 1969.

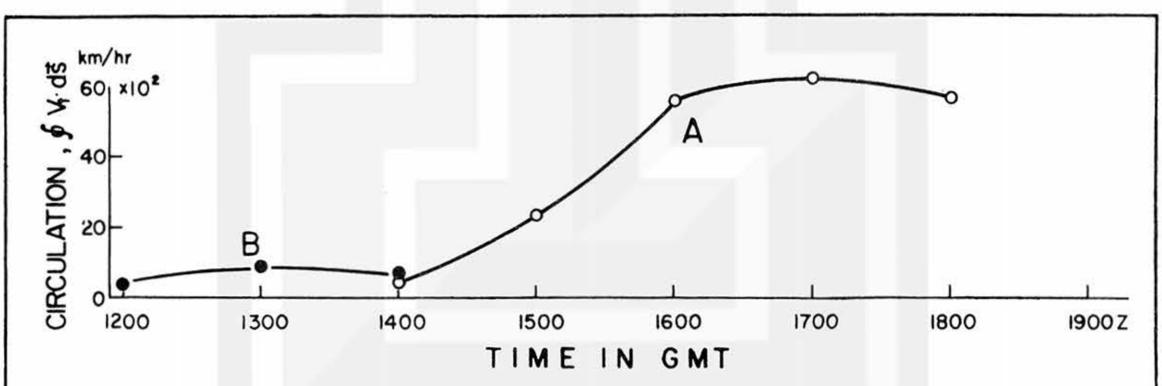

Fig. 10. The circulation along the boundaries of anvils A and B for July 26, 1969.

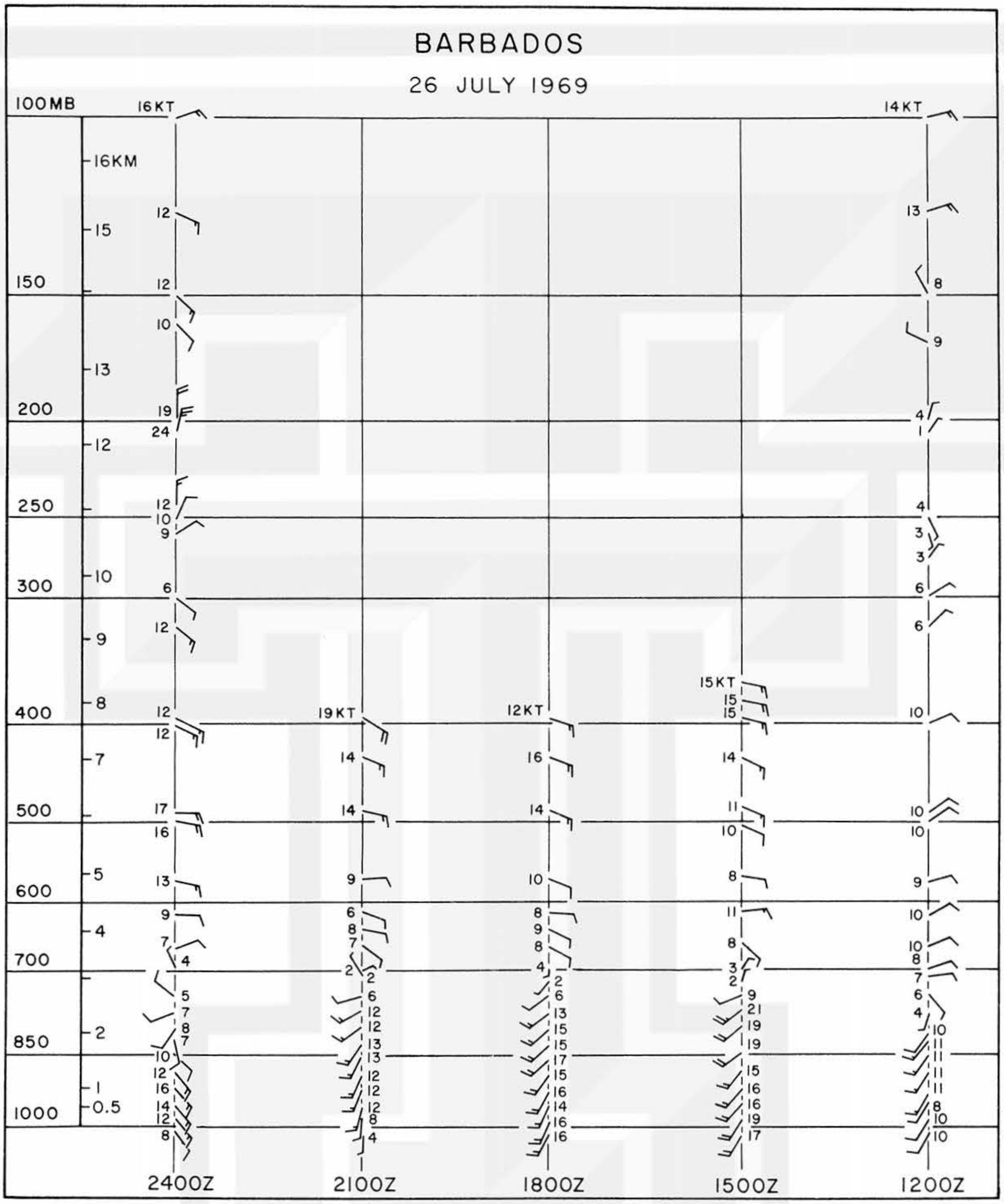

Fig. 11. Vertical time cross section of wind at Barbados for 1200, 1500, 18, 2100 and 2400 GMT, July 26, 1969.

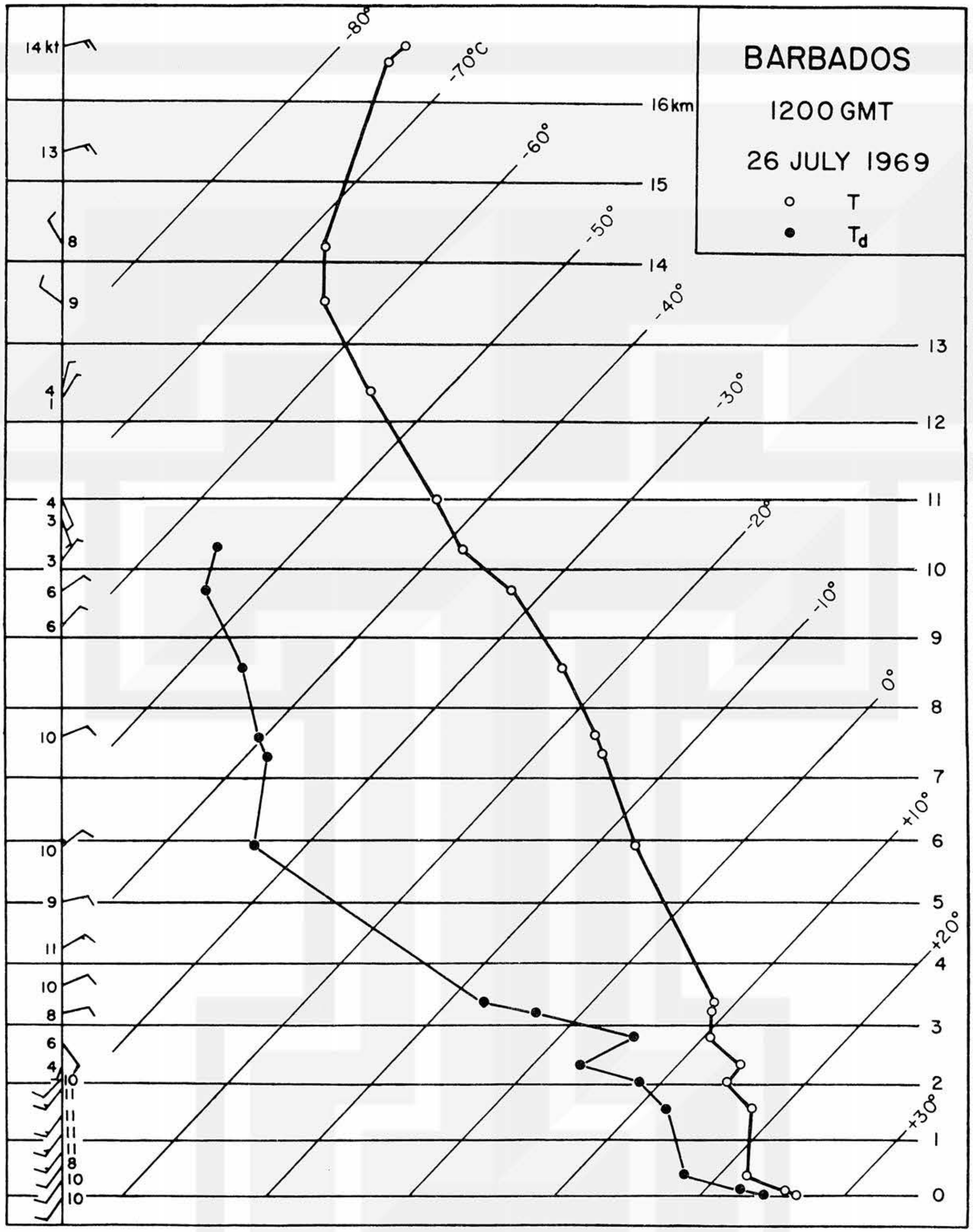

Fig. 12. The 1200 GMT rawinsonde at Barbados for July 26, 1969.

The growing anvils A and B, observed from the satellite pictures, can be considered as a consequence of the strong low-level convection produced in the large scale weather system discussed above, of which anvil B had much less strength compared with anvil A. The anticyclonic circulation shown in Fig. 10 is also, as expected, evidence of the anticyclone aloft. A maximum of outflow (see Fig. 9) and circulation of anvil A at 1600 Z reveal the full development of the weather system at that time. When the system passed during the late hours of the anvil growth period, there was a consequential decrease of outflow. The maximum growth or horizontal spreading that appears at the west edge of both anvils A and B is related not only to the large-scale easterlies but also to the westward movement of the large-scale weather system.

6. CONCLUSIONS

It has been shown that by tracking the anvil boundaries from a sequence of ATS picture enlargements near the Barbados area, reliable mean divergence and outflow fields at upper level can be obtained. Detailed analysis of the hourly anvil boundaries and cloud velocities over the anvil area reveals not only a close relation but also a good correspondence between the growth of the anvils and the existence and movement of a large-scale weather system. Although the anvil growth superimposed on the large-scale motion in the tropics is one of the small-scale disturbances, and since the large-scale motion is totally different from the cloud motion over the anvil area, it is thus suggested that the tracking of anvil boundaries could certainly give more understanding to the mechanism of tropical circulation.

However, more simultaneous upper-air observations at the anvil area are necessary to analyze and interpret the physics of the anvil growth. Further studies of anvil growth over the tropics are needed to investigate the interactions between small-scale convective disturbances and large-scale atmospheric circulation.

ACKNOWLEDGMENTS:-

The author wishes to acknowledge Professor T. T. Fujita for his discussions, encouragement and support. Also, the author is grateful to Mr. Jaime J. Tecson for his suggestions and for reading the manuscript.

REFERENCES

Chang, Y. M., J. J. Tecson, and T. T. Fujita (1973): METRACOM System of Cloud Velocity Determination from Geostationary Satellite Pictures. SMRP Research Paper 110, University of Chicago.

________ and J. J. Tecson (1974): Cloud Velocity Over the North Atlantic Computed from ATS Picture Sequences. SMRP Research Paper 121, University of Chicago.

Fernandez-Partagas, J. J. and M. A. Estoque (1970): A Preliminary Report on Meteorological Conditions During BOMEX, Fourth Phase (July 11-28, 1969). Rosenstiel School of Marine and Atmospheric Sciences, University of Miami.

Fujita, T. T. and D. L. Bradbury (1969): Determination of Mass Outflow from a Thunderstorm Complex Using ATS-III Pictures, 6th Conference on Severe Local Storms, Chicago, 38-43.

________(1974): Overshooting Thunderheads Observed From ATS and Learjet. SMRP Research Paper 117, University of Chicago.

Purdom, J. F. W. (1971): Satellite Imagery and Severe Weather Warning. 7th Conference on Severe Local Storms, Kansas City, 120-127.

Sikdar, D. N., V. E. Suomi and C. E. Anderson (1970): Convective Transport of Mass and Energy in Severe Storms Over the United States - - An Estimate From a Geostationary Altitude. Tellus XXII, 5, 521-522.

MESOMETEOROLOGY PROJECT - - - RESEARCH PAPERS

(Continued from front cover)

42.* A Study of Factors Contributing to Dissipation of Energy in a Developing Cumulonimbus - Rodger A. Brown and Tetsuya Fujita

43. A Program for Computer Gridding of Satellite Photographs for Mesoscale Research - William D. Bonner

44. Comparison of Grassland Surface Temperatures Measured by TIROS VII and Airborne Radiometers under Clear Sky and Cirriform Cloud Conditions - Ronald M. Reap

45. Death Valley Temperature Analysis Utilizing Nimbus I Infrared Data and Ground-Based Measurements - Ronald M. Reap and Tetsuya Fujita

46. On the "Thunderstorm-High Controversy" - Rodger A. Brown

47. Application of Precise Fujita Method on Nimbus I Photo Gridding - Lt. Cmd. Ruben Nasta

48. A Proposed Method of Estimating Cloud-top Temperature, Cloud Cover, and Emissivity and Whiteness of Clouds from Short- and Long-wave Radiation Data Obtained by TIROS Scanning Radiometers - T. Fujita and H. Grandoso

49. Aerial Survey of the Palm Sunday Tornadoes of April 11, 1965 - Tetsuya Fujita

50. Early Stage of Tornado Development as Revealed by Satellite Photographs - Tetsuya Fujita

51. Features and Motions of Radar Echoes on Palm Sunday, 1965 - D. L. Bradbury and T. Fujita

52. Stability and Differential Advection Associated with Tornado Development - Tetsuya Fujita and Dorothy L. Bradbury

53. Estimated Wind Speeds of the Palm Sunday Tornadoes - Tetsuya Fujita

54. On the Determination of Exchange Coefficients: Part II - Rotating and Nonrotating Convective Currents - Rodger A. Brown

55. Satellite Meteorological Study of Evaporation and Cloud Formation over the Western Pacific under the Influence of the Winter Monsoon - K. Tsuchiya and T. Fujita

56. A Proposed Mechanism of Snowstorm Mesojet over Japan under the Influence of the Winter Monsoon - T. Fujita and K. Tsuchiya

57. Some Effects of Lake Michigan upon Squall Lines and Summertime Convection - Walter A. Lyons

58. Angular Dependence of Reflection from Stratiform Clouds as Measured by TIROS IV Scanning Radiometers - A. Rabbe

59. Use of Wet-beam Doppler Winds in the Determination of the Vertical Velocity of Raindrops inside Hurricane Rainbands - T. Fujita, P. Black and A. Loesch

60. A Model of Typhoons Accompanied by Inner and Outer Rainbands - Tetsuya Fujita, Tatsuo Izawa., Kazuo Watanabe and Ichiro Imai

61. Three-Dimensional Growth Characteristics of an Orographic Thunderstorm System - Rodger A. Brown

62. Split of a Thunderstorm into Anticyclonic and Cyclonic Storms and their Motion as Determined from Numerical Model Experiments - Tetsuya Fujita and Hector Grandoso

63. Preliminary Investigation of Peripheral Subsidence Associated with Hurricane Outflow - Ronald M. Reap

64. The Time Change of Cloud Features in Hurricane Anna, 1961, from the Easterly Wave Stage to Hurricane Dissipation - James E. Arnold

65. Easterly Wave Activity over Africa and in the Atlantic with a Note on the Intertropical Convergence Zone during Early July 1961 - James E. Arnold

66. Mesoscale Motions in Oceanic Stratus as Revealed by Satellite Data - Walter A. Lyons and Tetsuya Fujita

67. Mesoscale Aspects of Orographic Influences on Flow and Precipitation Patterns - Tetsuya Fujita

68. A Mesometeorological Study of a Subtropical Mesocyclone -Hidetoshi Arakawa, Kazuo Watanabe, Kiyoshi Tsuchiya and Tetsuya Fujita

69. Estimation of Tornado Wind Speed from Characteristic Ground Marks - Tetsuya Fujita, Dorothy L. Bradbury and Peter G. Black

70. Computation of Height and Velocity of Clouds from Dual, Whole-Sky, Time-Lapse Picture Sequences - Dorothy L. Bradbury and Tetsuya Fujita

71. A Study of Mesoscale Cloud Motions Computed from ATS-I and Terrestrial Photographs - Tetsuya Fujita, Dorothy L. Bradbury, Clifford Murino and Louis Hull

72. Aerial Measurement of Radiation Temperatures over Mt. Fuji and Tokyo Areas and Their Application to the Determination of Ground- and Water-Surface Temperatures - Tetsuya Fujita, Gisela Baralt and Kiyoshi Tsuchiya

73. Angular Dependence of Reflected Solar Radiation from Sahara Measured by TIROS VII in a Torquing Maneuver - Rene Mendez.

74. The Control of Summertime Cumuli and Thunderstorms by Lake Michigan During Non-Lake Breeze Conditions - Walter A. Lyons and John W. Wilson

75. Heavy Snow in the Chicago Area as Revealed by Satellite Pictures - James Bunting and Donna Lamb

76. A Model of Typhoons with Outflow and Subsidence Layers - Tatsuo Izawa

* out of print

(continued on outside back cover)

77. Yaw Corrections for Accurate Gridding of Nimbus HRIR Data - R. A. Madden

78. Formation and Structure of Equatorial Anticyclones caused by Large-Scale Cross Equatorial Flows determined by ATS I Photographs - T. T. Fujita, K. Watanabe and T. Izawa

79. Determination of Mass Outflow from a Thunderstorm Complex using ATS III Pictures - T. T. Fujita and D. L. Bradbury

80. Development of a Dry Line as shown by ATS Cloud Photography and verified by Radar and Conventional Aerological Data - D. L. Bradbury

81. Dynamical Analysis of Outflow from Tornado-Producing Thunderstorms as revealed by ATS III Pictures - K. Ninomiya

*82. Computation of Cloud Heights from Shadow Positions through Single Image Photogrammetry of Apollo Pictures - T. T. Fujita

83. Aircraft, Spacecraft, Satellite and Radar Observations of Hurricane Gladys, 1968 - R. C. Gentry, T. Fujita and R. C. Sheets

84. Basic Problems on Cloud Identification related to the design of SMS-GOES Spin Scan Radiometers - T. T. Fujita

85. Mesoscale Modification of Synoptic Situations over the Area of Thunderstorms' Development as revealed by ATS III and Aerological Data - K. Ninomiya

86. Palm Sunday Tornadoes of April 11, 1965 - T. T. Fujita, D. L. Bradbury and C. F. Van Thullenar (Reprinted from Mon. Wea. Rev., 98, 29-69, 1970)

87. Patterns of Equivalent Blackbody Temperature and Reflectance of Model Clouds computed by changing Radiometer's Field of View - J. J. Tecson

88. Lubbock Tornadoes of 11 May 1970 - T. T. Fujita

89. Estimate of Areal Probability of Tornadoes from Inflationary Reporting of their Frequencies - T. T. Fujita

90. Application of ATS III Photographs for determination of Dust and Cloud Velocities over Northern Tropical Atlantic - T. T. Fujita

91. A Proposed Characterization of Tornadoes and Hurricanes by Area and Intensity - T. T. Fujita

92. Estimate of Maximum Wind Speeds of Tornadoes in Three Northwestern States - T. T. Fujita

93. In- and Outflow Field of Hurricane Debbie as revealed by Echo and Cloud Velocities from Airborne Radar and ATS-III Pictures - T. T. Fujita and P. G. Black (Reprinted from Preprint of Radar Meteorology Conference, Nov. 17-20, 1970, Tucson, Arizona)

94. Characterization of 1965 Tornadoes by their Area and Intensity - J. J. Tecson

*95. Computation of Height and Velocity of Clouds over Barbados from a Whole-Sky Camera Network - R. D. Lyons

96. The Filling over Land of Hurricane Camille, August 17-18, 1969 - D. L. Bradbury

97. Tornado Occurrences related to Overshooting Cloud-Top Heights as determined from ATS Pictures - T. T. Fujita

98. FPP Tornado Scale and its Applications - T. T. Fujita and A. D. Pearson

99. Preliminary Results of Tornado Watch Experiment 1971 - T. T. Fujita, J. J. Tecson and L. A. Schaal

100. F-Scale Classification of 1971 Tornadoes - T. T. Fujita

101. Typhoon-Associated Tornadoes in Japan and new evidence of Suction Vortices in a Tornado near Tokyo - T. T. Fujita

102. Proposed Mechanism of Suction Spots accompanied by Tornadoes - T. T. Fujita

103. A Climatological Study of Cloud Formation over the Atlantic during Winter Monsoon - H. Shitara

**104. Statistical Analysis of 1971 Tornadoes - E. W. Pearl

105. Estimate of Maximum Windspeeds of Tornadoes in Southernmost Rockies - T. T. Fujita

106. Use of ATS Pictures in Hurricane Modification - T. T. Fujita

107. Mesoscale Analysis of Tropical Latin America - T. T. Fujita

108. Tornadoes Around The World - T. T. Fujita (Reprinted from Weatherwise, 26, No. 2, April 1973)

109. A Study of Satellite-Observed Cloud Patterns of Tropical Cyclones - E. E. Balogun

110. METRACOM System of Cloud-Velocity determination from Geostationary Satellite Pictures - Y. M. Chang, J. J. Tecson and T. T. Fujita

111. Proposed Mechanism of Tornado Formation from Rotating Thunderstorm - T. T. Fujita

112. Joliet Tornado of April 6, 1972 - E. W. Pearl

113. Results of FPP Classification of 1971 and 1972 Tornadoes - T. T. Fujita and A. D. Pearson

114. Satellite-Tracked Cumulus Velocities - T. T. Fujita, E. W. Pearl and W. E. Shenk

115. General and Local Circulation of Mantle and Atmosphere toward Prediction of Earthquakes and Tornadoes - T. T. Fujita and K. Fujita

116. Cloud Motion Field of Hurricane Ginger during the Seeding Period as determined by the METRACOM System - J. J. Tecson, Y. M. Chang and T. T. Fujita

117. Overshooting Thunderheads observed from ATS and Learjet - T. T. Fujita

118. Thermal and Dynamical Features of a Thunderstorm with a Tilted Axis of Rotation - T. T. Fujita

119. Characteristics of Anvil-Top Associated with the Poplar Bluff Tornado of May 7, 1973 - E. W. Pearl

120. Jumbo Tornado Outbreak of 3 April 1974 - T. T. Fujita

121. Cloud Velocities Over The North Atlantic Computed From ATS Picture Sequences - Y. M. Chang and J. J. Tecson